Baseline and morphine-induced rat microglial phagocytic activity is regulated by sex, brain region, and density interactions *ex vivo*

David N. King'uyu[a], Lily Nti-Kyemereh[a,b], Michelle Tram[b], Ashley M. Kopec[a*]

a) Department of Neuroscience and Experimental Therapeutics
Albany Medical College
Albany, NY 12208

b) Siena College
Loudonville, NY 12211

*) Corresponding Author
43 New Scotland, NY 12208
kopeca@amc.edu

ABSTRACT

Opioids have long been used for clinical pain management, but also have addictive properties that have contributed to the ongoing opioid epidemic. While opioid activation of opioid receptors is well known to contribute to reward and reinforcement, data now also suggest that opioid activation of immune signaling via toll-like receptor 4 (TLR4) may also play a role in addiction-like processes. TLR4 expression is enriched in immune cells in peripheral organs and blood and in the nervous system is primarily expressed in microglia, the resident immune cells of the central nervous system. In peripheral immune cells, morphine is repeatedly shown to decreases immune activation and phagocytosis *in vivo* and *in vitro*. Phagocytosis is an important immune effector that serves to clear damage, debris, and infection. Unlike peripheral immune cells, the effect of morphine on microglia is less well studied. Morphine is reported to both increase and decrease microglial phagocytosis. Several different factors contribute to microglial phagocytic activity, including sex, region, and local microglial density. We hypothesized that morphine increases phagocytic activity in microglia, but in a density-, dose-, region-, and sex-dependent manner *ex vivo*. To test this, we isolated microglia from adult male and female rat cortex and striatum and plated them *ex vivo* at a relatively low or high density. Microglia were incubated with neutral fluorescent microbeads to stimulate phagocytosis in the presence of one of four morphine doses. We found that brain region of origination and plating density, but not sex, impacted microglial phagocytosis at baseline. These heterogenous properties further diverge when morphine is applied causing emergence of effects not observed at baseline, maintenance of some baseline effects, and disappearance of effects observed at baseline. Further work is necessary to identify the precise interactions and signaling that is dominant in different sex, region, and density contexts to better understand the complex effects of opioids on microglial immunoregulation.

Funding: This work was supported by the National Institutes of Health [R01DA052889 and R03AG07011) and Albany Medical College Start-up funds, all to AMK.

INTRODUCTION

Opioids have long been used for clinical pain management, but also have addictive properties (Agmo and Gómez 1991, Paredes 2014, Quintana, Mac Cionnaith et al. 2022) that have contributed to the ongoing opioid epidemic (Terplan 2017, Stoicea, Costa et al. 2019). The opioid morphine binds to both opioid receptors, which are present on several different cell types, and Toll-like Receptor 4 (TLR4), which is enriched on immune cells (Wang, Loram et al. 2012, Xie, Gomes et al. 2017). Opioid receptor and TLR4 have different intracellular signaling pathways. For example, in peripheral immune cells opioid receptor activation induces synthesis and release of opioid peptides (Schäfer, Carter et al. 1994, Boué, Blanpied et al. 2011), while TLR4 activation is generally pro-inflammatory and associated with cytokine release and phagocytic activity (Schaub, Bellou et al. 2004, Ninkovic, Anand et al. 2016). While opioid activation of opioid receptors is well known to contribute to reward and reinforcement, data now also suggest that opioid activation of TLR4 may play a role in addiction-like processes (Hutchinson, Northcutt et al. 2012). Thus, understanding the diverse actions of opioids on different cell types is important to develop strategies to mitigate their negative consequences.

TLR4 expression is enriched in immune cells in peripheral organs and blood (Zaal, Nota et al. 2017) and in the nervous system is primarily expressed in microglia, the resident immune cells of the central nervous system (Zhang, Chen et al. 2014, Zhang, Sloan et al. 2016). In peripheral immune cells, morphine is repeatedly shown to decreases immune activation and phagocytosis *in vivo* and *in vitro* (Rojavin, Szabo et al. 1993, Ninković and Roy 2012, Ninkovic, Anand et al. 2016) dependent on dose (Borman, Ciepielewski et al. 2009) and duration of exposure (Pagán, Figueroa et al. 2001). Phagocytosis is an important immune effector that serves to clear damage, debris, and infection (Andoh and Koyama 2021). Unlike peripheral immune cells, the effect of morphine on microglia is less well studied. Morphine is reported to both increase and decrease microglial phagocytosis (Peterson, Gekker et al. 1995, Sowa, Gekker et al. 1997, Lipovsky, Gekker et al. 1998, Mali and Novotny 2022). There is no consensus on the modulatory effect of morphine on microglia phagocytosis currently.

Several different factors contribute to microglial phagocytic activity, including sex, region, and local microglial density. For example, during neonatal development female microglia are more phagocytically active in the hippocampus (Nelson, Warden et al. 2017) and mature faster (Hanamsagar, Alter et al. 2017) than male microglia. Morphine increases the number of activated microglia in females compared to males which correlates to morphine analgesic effect in the periaqueductal gray (Doyle, Eidson et al. 2017). Morphine also leads to sex specific microglia polarization in the periaqueductal gray (Doyle, Eidson et al. 2017). There also appears to be heterogeneity in the transcriptional profile of cortical and striatal microglia (Grabert, Michoel et al. 2016). The *in vivo* density of microglia varies depending on brain region with the highest density in the substantia nigra (Lawson, Perry et al. 1990). Morphine decreases the number of microglia in the substantia nigra (Jokinen, Sidorova et al. 2018). Thus, the influence of opioids and specifically morphine on microglia is complex and not fully understood.

We hypothesized that morphine increases phagocytic activity in microglia, but in a density-, dose-, region-, and sex-dependent manner *ex vivo*. To test this, we isolated microglia from adult male and female rat cortex and striatum and plated them *ex vivo* at a relatively low or high density. Microglia were incubated with neutral fluorescent microbeads to stimulate phagocytosis

in the presence of one of four morphine doses (**Fig. 1**). We found that brain region of origination and plating density, but not sex, impacted microglial phagocytosis at baseline. When we added morphine, microglial phagocytosis was revealed to be regulated via complex interactions between independent variables.

METHODS

Animals

Young adult (P70-P90) male and female Sprague Dawley rats were purchased (Envigo) and group-housed with ad libitum access to food and water for at least 2 weeks. Conditions were kept at 23°C on a 12:12 light:dark cycle (lights on at 07:00) and cages were changed twice a week. Experiments and animal care were approved by the Institutional Animal Care and Use Committee at Albany Medical College.

Tissue collection and microglial isolations

Animals were euthanized by CO_2 anesthesia and exsanguination. Saline perfusion was performed before animals were decapitated and brains extracted. Each brain had cortex and striatum regions grossly dissected and separated for mechanical and enzymatic breakdown. Brain regions were minced using a razor into a gelatinous consistency while on a petri dish resting on wet ice. Minced brain tissue underwent enzymatic dissociation using the Neural Tissue Dissociation Kit (P) protocol (Mitenyi Biotec, 130-092-628) to isolate neural cells. Neural cells were incubated in CD11b+ magnetic microbeads (Miltenyi Biotec, CD11b/c Microbeads, rat, 130-105-634) and CD11b+ cells positively selected through a magnetic column to enrich for microglial cells. We will refer to CD11b+ cells hereafter as microglia.

Ex vivo microglial assays

Microglia were incubated in media (0.1% forskolin in Dubelco's Modified Eagle's Medium, 1% N2 media, 1% L-glutamine, 1% sodium pyruvate, 1% Pen-Strep) at 37 °C/5% CO_2 in chambered slides (Thermo Fisher Scientific Nunc Lab-Tek II CC^2 Chamber Slide, Z734853) at either relatively low 10K (10,000 cells/well or 50,000 cells/mL) and relatively high 50K (50,000 cells/well or 250,000 cells/mL) density. Cells were permitted to adhere to the chambered slides for 2hrs in media. Fluorescent microbeads (Polysciences Inc., Fluoresbrite Carboxylate YG 1.0-micron microspheres, 15702-10) and morphine sulfate (Mallinckrodt, H11662) at 0 Molar(M), 10^{-12} M, 10^{-8} M and 10^{-4} M were reconstituted in fresh media and added to seeded microglia. Cells were incubated at 37ºC for and additional 90mins to permit phagocytic activity as we have published (Kopec, Smith et al. 2018). Cells were rinsed with PBS, and paraformaldehyde (PFA; 4%) fixed.

Immunocytochemistry

Cells were blocked using 0.3% Triton x-100 in PBS, permeabilized using 10% donkey serum in Permeabilization buffer and stained using primary antibody 1:500 Iba1-rabbit (Wako; 019-19741) and incubated at 4ºC overnight. Cells were rinsed with PBS and incubated with secondary antibody 1:500 Alexa Fluor donkey anti-rabbit 568 (ThermoFisher, A21202) at room temperature for 2hrs in the dark the following day. Cells were rinsed and chambered slide well walls were removed leaving behind the glass slides on which cells adhered. Glass slides were allowed to dry overnight in the dark. Slides were cover slipped using mounting agent (Invitrogen, Prolong Glass Antifade Mountant, P36984) the following day.

Imaging and Data Acquisition

3-6 images per condition were captured on a ZEISS LSM 880 confocal microscope at 20x magnification to capture at least 20 cells per sample. 20µm slice z-stacks, 0.5µm step size, were taken of Texas Red (microglia) and GFP (microbeads) channels. Z-stacks were maximum projected into 2D images with ImageJ (National Institutes of Health; Bethesda, MD). Channels were separated and the microglia channel was manually outlined. Outlines were drawn by experimenters blinded to the experimental conditions. After all microglia in the image were outlined, cell outlines were overlayed onto the fluorescent microbead channel and mean gray value per microglia was calculated.

Statistical analysis

Independent variables were sex (male vs. female), region (cortex vs. striatum), density (10K vs. 50K), and morphine concentration (0, 10^{-12}, 10^{-8} and 10^{-4} M). Endpoints analyzed were (1) the proportion of microglia engaged in *any* phagocytic activity (binary) and (2) the amount of phagocytosed beads (continuous). Outliers were identified in Graphpad 9.4.1 using the ROUT method (Q set to 1%) and excluded. Statistics were performed in Minitab 21.1.0. To examine baseline effects in the vehicle-treated groups we performed a 3-way mixed model ANOVA (between: region x sex x density; random factor: animal). To examine the effect of morphine, we performed a four-way mixed model ANOVA (between: sex X region x density; within: morphine concentration; random factor: animal). Statistically significant F values ($p<0.05$) were followed by Tukey's post hoc tests. Figures were created in Graphpad 9.4.1. Within-group individual differences at baseline were evident, thus for ease of visual interpretation we depict the data normalized to low density striatum data for each animal for morphine analyses. Data analysis was performed on raw, non-normalized data.

RESULTS

We analyzed the data using two different measures: proportion of phagocytosing cells and amount of phagocytosed beads. The proportion of phagocytosis is a binary measure of microglia engaged in *any* phagocytic activity. Amount of phagocytosed beads is a measure of the bead fluorescent intensity within microglia, and represents microbead internalization.

Density, region, and sex influence basal phagocytic properties in isolated rat microglia

To determine whether density, region and sex impact the proportion of microglia engaged in phagocytosis at baseline, we first examined our vehicle control groups (**Fig. 2**). For the proportion of microglia engaged in phagocytosis (**Fig. 2A,B**), a main effect of region indicated that a higher proportion of cortical microglia were phagocytosing relative to striatal microglia. A sex by region interaction indicated that a higher proportion of female but not male cortical microglia were phagocytosing than striatal microglia. Finally, a main effect of density indicated that microglia cultured at 50K were proportionally more phagocytic.

With respect to the average amount of phagocytosed beads at baseline, there was only a main effect of region (**Fig. 2C,D**). The amount of phagocytosis was greater in the cortical microglia than in striatal microglia. Unlike the proportion of microglia engaged in phagocytosis, average amount of phagocytosis was not statistically significantly impacted by density or sex, though there are trends towards significance ($p < 0.1$) for a main effect of density and a density by

region interaction.

Morphine modulates the influence of density, region, and sex on phagocytic properties in isolated rat microglia

To determine whether morphine modulated the proportion of microglia engaged in phagocytosis in a density-, region-, and/or sex-specific manner we added 0M (vehicle control; data analyzed in Fig. 2), 10^{-12} M, 10^{-8} M, or 10^{-4} M morphine to *ex vivo* isolated rat microglia concurrent with fluorbead incubation. There were statistically significant main effects of drug and region on the proportion of microglia engaged in phagocytosis (**Fig. 3A,B**). Microglia exposed to 10^{-12} morphine were more likely to be engaged in phagocytosis than in microglia exposed to 0 M and 10^{-4} M. Additionally, a greater proportion of cortical microglia were engaged in phagocytosis than in striatal microglia, which was also evident in baseline data (**Fig. 2A,B**).

We next analyzed whether morphine modulated the average amount of phagocytosed beads in a density-, region-, and/or sex-specific manner. There were statistically significant effects of region, density, drug and interactions between sex and density as well as sex, region, and density (**Fig. 4A,B**). Similar to our observations at baseline (**Fig. 2C,D**), cortical microglia had a significantly greater amount of phagocytosed beads per microglia compared to striatal microglia. The addition of morphine as a variable also stimulated statistically significant effects not observed at baseline. Microglia at a higher density had a significantly greater amount of phagocytosed beads compared to microglia at a lower density. Microglia exposed to10^{-12} M morphine had a significantly greater amount of phagocytosed beads than all other concentrations. Male microglia cultured at a high density had a greater amount of phagocytosed beads than male microglia cultured at a lower density. The three-way sex by region by density interaction further revealed that male cortical microglia cultured at a high density had a greater amount of phagocytosed beads than both lower density cortical male microglia and striatal male microglia at either density. Finally, female cortical microglia cultured at either density had a greater amount of phagocytosed beads than female striatal microglia at either density.

DISCUSSION

Herein, we demonstrate that sex, cortical vs. striatal region of isolation, and culture density impact baseline phagocytic responses in microglia. Morphine exposure increases phagocytic responses in a dose-dependent manner and reveals density-, region-, and sex-dependent effects that are not present at baseline (**Fig. 5**).

The effects of sex, density and region on microglial phagocytic activity

Sex specific transcriptional profiles of microglia have been observed in different brain regions and age points. Therefore, we expected to find main effects of sex. We did not find a main effect of sex at baseline nor in the presence of morphine in any of our endpoints. Instead, at baseline the proportion of microglia engaged in phagocytosis varied via a sex by region interaction, in which female cortical microglia were more likely to be phagocytosing than female striatal microglia (**Fig. 2A,B**). However, the effect of sex did not modulate the proportion of microglia engaged in phagocytosis when morphine was present. The stimulatory main effect of morphine was sufficient to occlude this female regional difference (**Fig. 3**). These data may suggest that female striatal microglia can engage in phagocytic activity if stimulated appropriately, or alternatively, female cortical microglia may be in a more basally active state.

While there was no effect of sex in amount of phagocytosis at baseline (**Fig. 1C,D**), the presence of morphine reveals a sex by density and a sex by region by density interaction (**Fig. 4**). Female cortical microglia at either density had a higher amount of phagocytosis than female striatal microglia. Unlike the proportion of microglia engaged in phagocytosis, which was modulated in females only, both male and female sex modulated phagocytic activity in the presence of morphine. In males, there was a higher amount of phagocytosis occurring in microglia at a 50K density than at a 10K density. Male cortical microglia plated at 50K also had a higher amount of phagocytosis than male cortical microglia at 10K or male striatal microglia at either density. We suspect that high inter-individual variability occluded the effect of density at baseline, while morphine exacerbated its impact, thus revealing it. This suggests that morphine may potentiate inter-cellular signaling that contributes to phagocytic capacity. Morphine potentiates synthesis and release of IL-1β, and TNF-α and ERK signaling in microglia (Liang, Chu et al. 2016, Yang, Sun et al. 2021) which are relevant for microglia activation. The interaction between sex, region, and density suggests that male cortical microglia specifically may be more responsive to intercellular signaling. Taken together, sex does appear to be an important factor but gains robustness when effects are interacting with other factors.

There was a main effect of region in both endpoints, and at both baseline and in the presence of morphine. To our surprise, cortical microglia were more likely to be engaged in phagocytosis and had higher average amounts of phagocytosed beads. Microglial heterogeneity is observed in basal ganglia microglia to begin as early as postnatal week two (De Biase, Schuebel et al. 2017). Microglia in the two regions we looked at may have differences in these processes that make cortical microglia capable of higher phagocytic capacity than striatum. The mechanisms behind the greater cortex phagocytic effects are unclear because of the multiple brain regions encompassed by delineation of tissue into such a global binary characterization (cortex and striatum).

The effects of morphine on microglial phagocytic activity

There was a main effect of morphine, with 10^{-12} M morphine increasing both the proportion of microglia engaged in phagocytosis (**Fig. 3**) as well as the amount of phagocytosis (**Fig. 4**). Importantly, these data indicate that striatal microglia, which are less phagocytically active than cortical microglia in these measurements, are *capable* of phagocytic engagement, and not simply sustaining higher adverse effects or attrition from isolation protocols. We probed both lower and higher concentrations of morphine and found a dose-dependent response. Opioid and TLR4 receptors influence morphine effects on microglia immune signaling (Wang, Loram et al. 2012, Liang, Chu et al. 2016, Xie, Gomes et al. 2017, Yang, Sun et al. 2021). Opioids engage these receptors to modulate phagocytosis in microglia (Lipovsky, Gekker et al. 1998). In peripheral macrophages TLR4 potentiates phagocytosis more robustly than opioid receptors (Ninkovic, Anand et al. 2016). If this is also true in microglia, our observations suggest that the TLR4-morphine interaction might be dominant at lower concentrations thereby enhancing phagocytosis.

Morphine penetrance into the brain is dependent on the dose, route of administration, metabolism, and inter-individual factors (Smith 2009, Rogers, Mehta et al. 2013, Chaves, Remiao et al. 2017, Ollikainen, Aitta-Aho et al. 2019). We find that at lower morphine

concentration regimes phagocytosis is increased. This suggests that there is a window of increased microglia phagocytosis *in vivo* which could be immediate or delayed based on peak brain morphine concentration as the concentration decays with time.

The effects of inter-individual variability on microglial phagocytic activity

In **Figs. 3-4**, to visualize the effects of sex, region, and density in the context of a morphine exposure, we normalized the data to the striatal 10K condition for each animal. We did this because of the level of inter-individual variability observed at baseline (displayed in **Fig. 2**), particularly in the amount of phagocytosis. These data indicate that microglia from different rats have heterogeneous phagocytic profiles. However, data from rats with higher phagocytic profiles at baseline still varied by sex, region, density, and morphine concentration like animals with lower phagocytic profiles at baseline, which can better be observed in the normalized data. Deep single cell RNA sequencing reveals that microglia transcriptomes are heterogenous (Li, Cheng et al. 2019) and developmental origin of microglia subpopulations is different (De, Van Deren et al. 2018) indicating features that may underlie microglia variability across a population (Yang, Onos et al. 2021). Further, while there are several statistically significant main effects present in these data, there are also cases in which visual inspection tells a different story. For example, in **Fig. 4A**, 10K cortical male microglia did not really respond to morphine at any concentration. And, there was no real effect of density on female striatal microglia. These nuances can be occluded in a large statistical dataset, but may very well be important.

Conclusion

We have demonstrated that *ex vivo* microglia have heterogenous phagocytosis properties. These heterogenous properties further diverge when morphine is applied causing emergence of effects not observed at baseline, maintenance of some baseline effects, and disappearance of effects observed at baseline. Further work is necessary to identify the precise interactions and signaling that is dominant in different sex, region, and density contexts to better understand the complex effects of opioids on microglial immunoregulation.

Acknowledgements: We thank Dr. Justin Bourgeois for analysis assistance and Dr. Paul Feustel for statistical consultation.

Author Declarations: DNK, LN, and AMK designed, performed, and analyzed the experiments. DNK, MT, and AMK wrote the manuscript. All authors edited the manuscript. The authors declare no conflicts of interest.

FIGURES

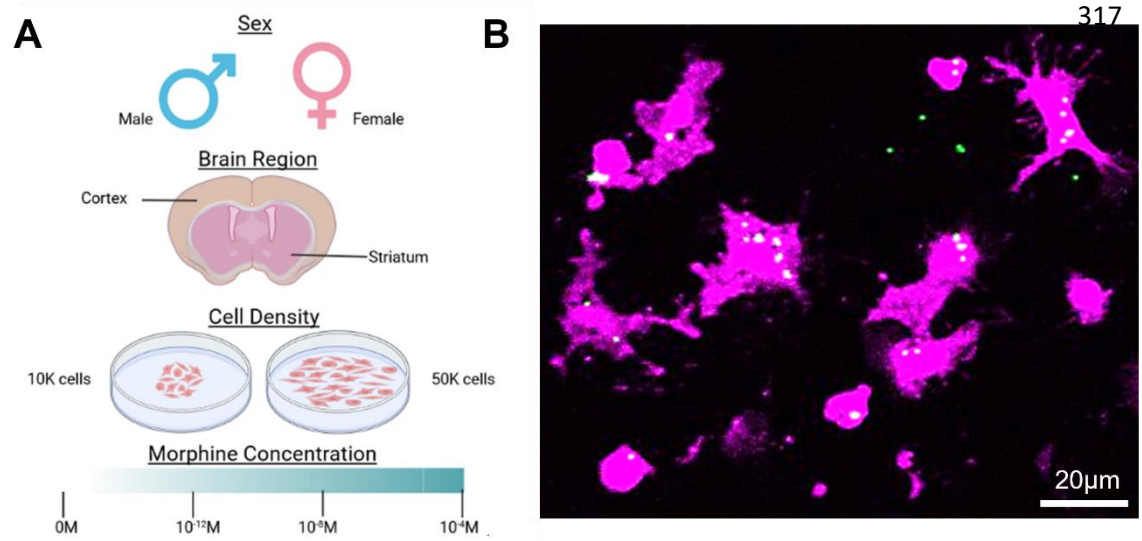

Figure 1: Experimental Design

(A) Experimental design included sex (male vs. female), brain region (cortex vs. striatum), density (low (10,000 microglia/well) vs. high (50,000 microglia/well), and morphine concentration (0, 10^{-12}, 10^{-8}, and 10^{-4} M) as independent variables. **(B)** Representative image of Iba1+ microglia (magenta) and fluorbeads (green).

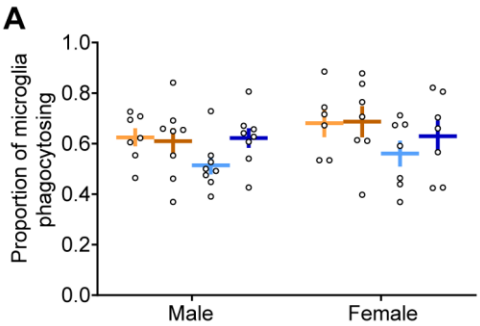

B

Baseline Proportion of Microglia Phagocytosing

Comparison	F Statistic	p-value	Tukey's posthoc
Sex	0.05	0.827	
Region	17.40	>0.001	Cortex > Striatum
Density	6.52	0.015	50K > 10K
Sex x Region	5.61	0.024	Female Cortex > Female Striatum
Sex x Density	2.29	0.139	
Region x Density	0.02	0.888	
Sex x Region x Density	0.59	0.448	

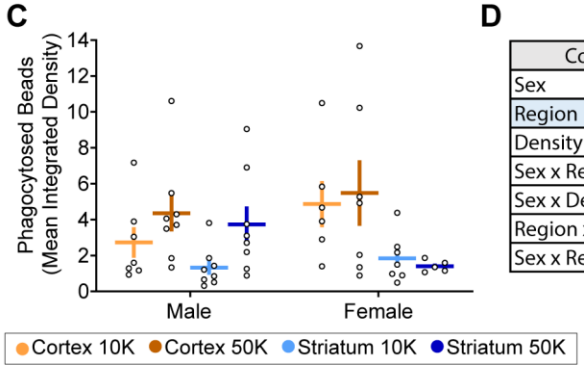

D

Baseline Phagocytosed Beads

Comparison	F Statistic	p-value	Tukey's posthoc
Sex	0.31	0.590	
Region	14.37	0.001	Cortex > Striatum
Density	3.99	0.054	
Sex x Region	2.17	0.150	
Sex x Density	0.06	0.815	
Region x Density	3.29	0.079	
Sex x Region x Density	1.15	0.292	

Figure 2: Density, region, and sex influence proportion of phagocytosis and phagocytosed beads at baseline

Striatal or cortical microglia were extracted from adult male and female rats, plated at 10K or 50K densities, and fed fluor beads. **(A)** Region and microglial density significantly impacted the proportion of phagocytosing microglia. Proportion of phagocytosis was greater in cortex than striatum and 50K was greater than 10K respectively. Additionally, there was a statistically significant interaction of Sex x Region and variance in female cortex was greater than female striatum. **(B)** Three-way mixed model ANOVA summary statistics: light blue highlighted rows indicate statistically significant results. **(C)** There was a statistically significant main effect of region in baseline variance of magnitude of phagocytosis. Cortex had greater variance of phagocytosis magnitude than striatum. **(D)** Three-way mixed model ANOVA summary statistics: light blue highlighted rows indicate statistically significant results. For all data, $p<0.05$ is defined as statistically significant. n = 6-8 rats/group. Horizontal lines depict average, vertical lines depict standard error of the mean.

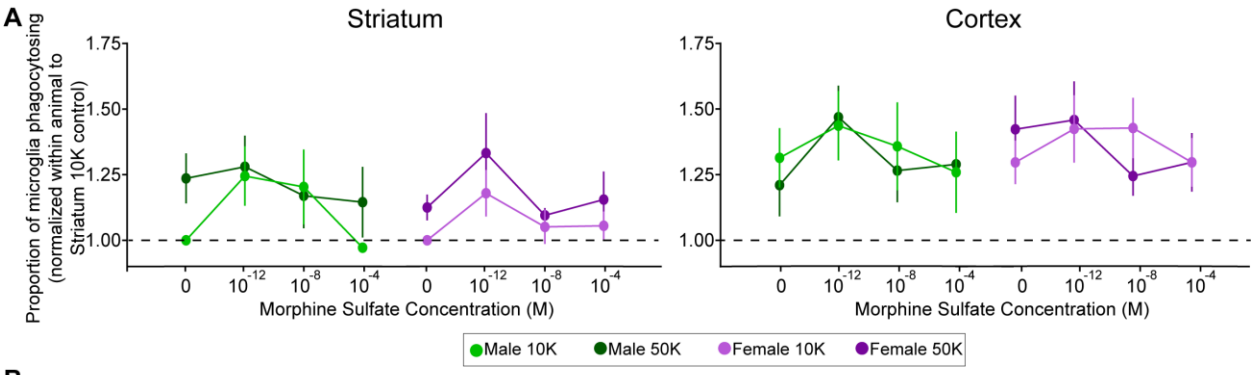

B

Comparison	F Statistic	p-value	Tukey's posthoc
Sex	0.61	0.450	
Region	35.37	>0.001	Cortex > Striatum
Density	3.19	0.076	
Drug	5.57	0.001	10^{-12}M > 0M, 10^{-4}M
Sex x Region	1.71	0.193	
Sex x Density	0.01	0.910	
Sex x Drug	0.13	0.944	
Region x Density	2.72	0.101	
Region x Drug	0.01	0.999	
Density x Drug	0.54	0.657	
Sex x Region x Density	1.03	0.311	
Sex x Region x Drug	0.40	0.751	
Sex x Density x Drug	0.10	0.961	
Region x Density x Drug	0.45	0.719	
Sex x Region x Density x Drug	0.74	0.528	

Figure 3. Morphine modulates the influence of density, region, and sex on proportion of microglia engaged in phagocytosis.
Striatal or cortical microglia were extracted from adult male and female rats, plated at 10K or 50K densities, and incubated with fluorbeads and morphine. Significant differences at baseline values were evident, thus for ease of visual data were normalized to 10K striatum for each animal. Data analysis was performed on raw, non-normalized data. **(A)** There were statistically significant main effects of region and drug. Proportion of microbead phagocytosis was greater in cortex than in striatum and 10^{-12}M morphine concentration was greater than 10M, 10^{-4}M respectively. **(B)** Four-way mixed model ANOVA summarized statistics table; light blue highlighted rows indicate statistically significant results. There were not statistically significant interactions. Post hoc tests were performed with Tukey's post hoc test; $p<0.05$ is defined as statistically significant. n = 6-8 rats/group. Circles depict average, vertical lines depict standard error of the mean.

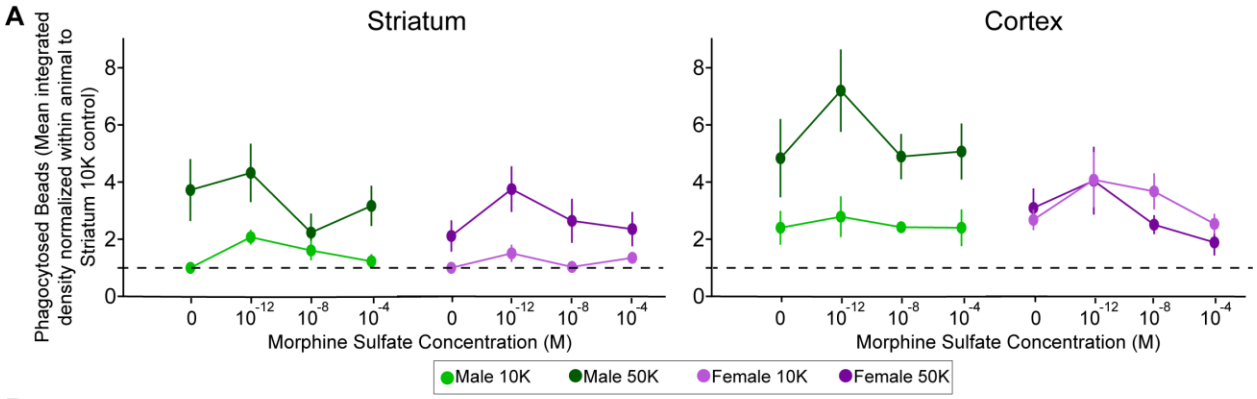

B

Comparison	F Statistic	p-value	Tukey's posthoc
Sex	0.11	0.747	
Region	50.73	>0.001	Cortex > Striatum
Density	19.40	>0.001	50K > 10K
Drug	10.32	>0.001	10^{-12}M > all others
Sex x Region	2.05	0.154	
Sex x Density	8.89	0.003	Male 50K > Male 10K
Sex x Drug	0.10	0.962	
Region x Density	0.14	0.712	
Region x Drug	1.37	0.253	
Density x Drug	0.83	0.479	
Sex x Region x Density	4.65	0.032	Male Cortex 50K > Male Striatum (10K and 50K), Male Cortex 10K Female Cortex (10K and 50K) > Female Striatum (10K and 50K)
Sex x Region x Drug	1.28	0.282	
Sex x Density x Drug	0.32	0.810	
Region x Density x Drug	0.50	0.683	
Sex x Region x Density x Drug	1.97	0.120	

Figure 4: Morphine modulates influence of density, region, and sex on amount of phagocytosed beads.

Striatal or cortical microglia were extracted from adult male and female rats, plated at 10K or 50K densities, and incubated with fluorbeads and morphine. Significant differences at baseline values were evident, thus for ease of visual data were normalized to 10K striatum for each animal. Data analysis was performed on raw, non-normalized data. **(A)** There were statistically significant main effects of region, density, and drug. Magnitude of microbead phagocytosis was greater in cortex than in striatum, 50K was greater than 10K, and 10^{-12}M morphine concentration was greater than all other concentrations respectively. Furthermore, there were statistically significant two-way and three-way interactions of Sex x Density and Sex x Region x Density respectively. In Sex x Density male 50K was greater than male 10K and in Sex x Region x Density male cortex 50K was greater than all other male cortex and striatum conditions while female cortex 10K and 50K was greater than female striatum 10K and 50K. **(B)** Four-way mixed model ANOVA summary statistics; light blue highlighted rows indicate statistically significant results. Post hoc tests were performed with Tukey's post hoc test; $p<0.05$ is defined as statistically significant. n = 6-8 rats/group; Circles depict average, vertical lines depict standard error of the mean.

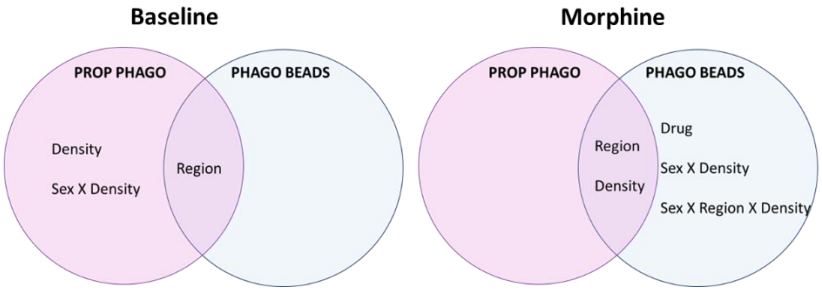

Figure 5: Venn diagrams of significant effects and interactions at baseline and with morphine.
Significant effects from Figs. 2-4 are summarized. Prop Phago = proportion of microglia engaged in phagocytosis; Phago Beads = Amount of phagocytosed bead signal.

455 **REFERENCES**

456 Agmo, A. and M. Gómez (1991). "Conditioned place preference produced by infusion of Met-enkephalin
457 into the medial preoptic area." Brain Res **550**(2): 343-346.
458 Andoh, M. and R. Koyama (2021). "Comparative Review of Microglia and Monocytes in CNS
459 Phagocytosis." Cells **10**(10).
460 Borman, A., Z. Ciepielewski, D. Wrona, W. Stojek, W. Glac, E. Leszkowicz and J. Tokarski (2009). "Small
461 doses of morphine can enhance NK cell cytotoxicity in pigs." Int Immunopharmacol **9**(3): 277-283.
462 Boué, J., C. Blanpied, P. Brousset, N. Vergnolle and G. Dietrich (2011). "Endogenous opioid-mediated
463 analgesia is dependent on adaptive T cell response in mice." J Immunol **186**(9): 5078-5084.
464 Chaves, C., F. Remiao, S. Cisternino and X. Decleves (2017). "Opioids and the Blood-Brain Barrier: A
465 Dynamic Interaction with Consequences on Drug Disposition in Brain." Curr Neuropharmacol **15**(8):
466 1156-1173.
467 De Biase, L. M., K. E. Schuebel, Z. H. Fusfeld, K. Jair, I. A. Hawes, R. Cimbro, H. Y. Zhang, Q. R. Liu, H. Shen,
468 Z. X. Xi, D. Goldman and A. Bonci (2017). "Local Cues Establish and Maintain Region-Specific Phenotypes
469 of Basal Ganglia Microglia." Neuron **95**(2): 341-356.e346.
470 De, S., D. Van Deren, E. Peden, M. Hockin, A. Boulet, S. Titen and M. R. Capecchi (2018). "Two distinct
471 ontogenies confer heterogeneity to mouse brain microglia." Development **145**(13).
472 Doyle, H. H., L. N. Eidson, D. M. Sinkiewicz and A. Z. Murphy (2017). "Sex Differences in Microglia Activity
473 within the Periaqueductal Gray of the Rat: A Potential Mechanism Driving the Dimorphic Effects of
474 Morphine." J Neurosci **37**(12): 3202-3214.
475 Grabert, K., T. Michoel, M. H. Karavolos, S. Clohisey, J. K. Baillie, M. P. Stevens, T. C. Freeman, K. M.
476 Summers and B. W. McColl (2016). "Microglial brain region-dependent diversity and selective regional
477 sensitivities to aging." Nat Neurosci **19**(3): 504-516.
478 Hanamsagar, R., M. D. Alter, C. S. Block, H. Sullivan, J. L. Bolton and S. D. Bilbo (2017). "Generation of a
479 microglial developmental index in mice and in humans reveals a sex difference in maturation and
480 immune reactivity." Glia **65**(9): 1504-1520.
481 Hutchinson, M. R., A. L. Northcutt, T. Hiranita, X. Wang, S. S. Lewis, J. Thomas, K. van Steeg, T. A.
482 Kopajtic, L. C. Loram, C. Sfregola, E. Galer, N. E. Miles, S. T. Bland, J. Amat, R. R. Rozeske, T. Maslanik, T.
483 R. Chapman, K. A. Strand, M. Fleshner, R. K. Bachtell, A. A. Somogyi, H. Yin, J. L. Katz, K. C. Rice, S. F.
484 Maier and L. R. Watkins (2012). "Opioid activation of toll-like receptor 4 contributes to drug
485 reinforcement." J Neurosci **32**(33): 11187-11200.
486 Jokinen, V., Y. Sidorova, H. Viisanen, I. Suleymanova, H. Tiilikainen, Z. Li, T. O. Lilius, K. Mätlik, J. E.
487 Anttila, M. Airavaara, L. Tian, P. V. Rauhala and E. A. Kalso (2018). "Differential Spinal and Supraspinal
488 Activation of Glia in a Rat Model of Morphine Tolerance." Neuroscience **375**: 10-24.
489 Kopec, A. M., C. J. Smith, N. R. Ayre, S. C. Sweat and S. D. Bilbo (2018). "Microglial dopamine receptor
490 elimination defines sex-specific nucleus accumbens development and social behavior in adolescent
491 rats." Nat Commun **9**(1): 3769.
492 Lawson, L. J., V. H. Perry, P. Dri and S. Gordon (1990). "Heterogeneity in the distribution and morphology
493 of microglia in the normal adult mouse brain." Neuroscience **39**(1): 151-170.
494 Li, Q., Z. Cheng, L. Zhou, S. Darmanis, N. F. Neff, J. Okamoto, G. Gulati, M. L. Bennett, L. O. Sun, L. E.
495 Clarke, J. Marschallinger, G. Yu, S. R. Quake, T. Wyss-Coray and B. A. Barres (2019). "Developmental
496 Heterogeneity of Microglia and Brain Myeloid Cells Revealed by Deep Single-Cell RNA Sequencing."
497 Neuron **101**(2): 207-223.e210.
498 Liang, Y., H. Chu, Y. Jiang and L. Yuan (2016). "Morphine enhances IL-1β release through toll-like
499 receptor 4-mediated endocytic pathway in microglia." Purinergic Signal **12**(4): 637-645.
500 Lipovsky, M. M., G. Gekker, S. Hu, A. I. Hoepelman and P. K. Peterson (1998). "Morphine enhances
501 complement receptor-mediated phagocytosis of Cryptococcus neoformans by human microglia." Clin
502 Immunol Immunopathol **87**(2): 163-167.

503 Mali, A. S. and J. Novotny (2022). "Opioid receptor activation suppresses the neuroinflammatory
504 response by promoting microglial M2 polarization." Mol Cell Neurosci **121**: 103744.
505 Nelson, L. H., S. Warden and K. M. Lenz (2017). "Sex differences in microglial phagocytosis in the
506 neonatal hippocampus." Brain Behav Immun **64**: 11-22.
507 Ninkovic, J., V. Anand, R. Dutta, L. Zhang, A. Saluja, J. Meng, L. Koodie, S. Banerjee and S. Roy (2016).
508 "Differential effects of gram-positive and gram-negative bacterial products on morphine induced
509 inhibition of phagocytosis." Sci Rep **6**: 21094.
510 Ninković, J. and S. Roy (2012). "Morphine decreases bacterial phagocytosis by inhibiting actin
511 polymerization through cAMP-, Rac-1-, and p38 MAPK-dependent mechanisms." Am J Pathol **180**(3):
512 1068-1079.
513 Ollikainen, E., T. Aitta-Aho, M. Koburg, R. Kostiainen and T. Sikanen (2019). "Rapid analysis of
514 intraperitoneally administered morphine in mouse plasma and brain by microchip electrophoresis-
515 electrochemical detection." Sci Rep **9**(1): 3311.
516 Pagán, W. E., N. Y. Figueroa and F. L. Renaud (2001). "Self-enhancement of phagocytosis by murine
517 resident peritoneal macrophages and its relationship to morphine effects on the process." Adv Exp Med
518 Biol **493**: 111-116.
519 Paredes, R. G. (2014). "Opioids and sexual reward." Pharmacol Biochem Behav **121**: 124-131.
520 Peterson, P. K., G. Gekker, S. Hu, W. S. Sheng, T. W. Molitor and C. C. Chao (1995). "Morphine stimulates
521 phagocytosis of Mycobacterium tuberculosis by human microglial cells: involvement of a G protein-
522 coupled opiate receptor." Adv Neuroimmunol **5**(3): 299-309.
523 Quintana, G. R., C. E. Mac Cionnaith and J. G. Pfaus (2022). "Behavioral, Neural, and Molecular
524 Mechanisms of Conditioned Mate Preference: The Role of Opioids and First Experiences of Sexual
525 Reward." Int J Mol Sci **23**(16).
526 Rogers, E., S. Mehta, R. Shengelia and M. C. Reid (2013). "Four Strategies for Managing Opioid-Induced
527 Side Effects in Older Adults." Clin Geriatr **21**(4).
528 Rojavin, M., I. Szabo, J. L. Bussiere, T. J. Rogers, M. W. Adler and T. K. Eisenstein (1993). "Morphine
529 treatment in vitro or in vivo decreases phagocytic functions of murine macrophages." Life Sci **53**(12):
530 997-1006.
531 Schäfer, M., L. Carter and C. Stein (1994). "Interleukin 1 beta and corticotropin-releasing factor inhibit
532 pain by releasing opioids from immune cells in inflamed tissue." Proc Natl Acad Sci U S A **91**(10): 4219-
533 4223.
534 Schaub, B., A. Bellou, F. K. Gibbons, G. Velasco, M. Campo, H. He, Y. Liang, M. W. Gillman, D. Gold, S. T.
535 Weiss, D. L. Perkins and P. W. Finn (2004). "TLR2 and TLR4 stimulation differentially induce cytokine
536 secretion in human neonatal, adult, and murine mononuclear cells." J Interferon Cytokine Res **24**(9):
537 543-552.
538 Smith, H. S. (2009). "Opioid metabolism." Mayo Clin Proc **84**(7): 613-624.
539 Sowa, G., G. Gekker, M. M. Lipovsky, S. Hu, C. C. Chao, T. W. Molitor and P. K. Peterson (1997).
540 "Inhibition of swine microglial cell phagocytosis of Cryptococcus neoformans by femtomolar
541 concentrations of morphine." Biochem Pharmacol **53**(6): 823-828.
542 Stoicea, N., A. Costa, L. Periel, A. Uribe, T. Weaver and S. D. Bergese (2019). "Current perspectives on the
543 opioid crisis in the US healthcare system: A comprehensive literature review." Medicine (Baltimore)
544 **98**(20): e15425.
545 Terplan, M. (2017). "Women and the opioid crisis: historical context and public health solutions." Fertil
546 Steril **108**(2): 195-199.
547 Wang, X., L. C. Loram, K. Ramos, A. J. de Jesus, J. Thomas, K. Cheng, A. Reddy, A. A. Somogyi, M. R.
548 Hutchinson, L. R. Watkins and H. Yin (2012). "Morphine activates neuroinflammation in a manner
549 parallel to endotoxin." Proc Natl Acad Sci U S A **109**(16): 6325-6330.
550 Xie, N., F. P. Gomes, V. Deora, K. Gregory, T. Vithanage, Z. D. Nassar, P. J. Cabot, D. Sturgess, P. N. Shaw

551 and M. O. Parat (2017). "Activation of μ-opioid receptor and Toll-like receptor 4 by plasma from
552 morphine-treated mice." Brain Behav Immun **61**: 244-258.
553 Yang, H. S., K. D. Onos, K. Choi, K. J. Keezer, D. A. Skelly, G. W. Carter and G. R. Howell (2021). "Natural
554 genetic variation determines microglia heterogeneity in wild-derived mouse models of Alzheimer's
555 disease." Cell Rep **34**(6): 108739.
556 Yang, Y., Y. Sun, R. Hu, J. Yan, Z. Wang, W. Li and H. Jiang (2021). "Morphine promotes microglial
557 activation by upregulating the EGFR/ERK signaling pathway." PLoS One **16**(9): e0256870.
558 Zaal, A., B. Nota, K. S. Moore, M. Dieker, S. M. van Ham and A. Ten Brinke (2017). "TLR4 and C5aR
559 crosstalk in dendritic cells induces a core regulatory network of RSK2, PI3Kβ, SGK1, and FOXO
560 transcription factors." J Leukoc Biol **102**(4): 1035-1054.
561 Zhang, Y., K. Chen, S. A. Sloan, M. L. Bennett, A. R. Scholze, S. O'Keeffe, H. P. Phatnani, P. Guarnieri, C.
562 Caneda, N. Ruderisch, S. Deng, S. A. Liddelow, C. Zhang, R. Daneman, T. Maniatis, B. A. Barres and J. Q.
563 Wu (2014). "An RNA-sequencing transcriptome and splicing database of glia, neurons, and vascular cells
564 of the cerebral cortex." J Neurosci **34**(36): 11929-11947.
565 Zhang, Y., S. A. Sloan, L. E. Clarke, C. Caneda, C. A. Plaza, P. D. Blumenthal, H. Vogel, G. K. Steinberg, M.
566 S. Edwards, G. Li, J. A. Duncan, 3rd, S. H. Cheshier, L. M. Shuer, E. F. Chang, G. A. Grant, M. G. Gephart
567 and B. A. Barres (2016). "Purification and Characterization of Progenitor and Mature Human Astrocytes
568 Reveals Transcriptional and Functional Differences with Mouse." Neuron **89**(1): 37-53.

569